Solid-state reaction induced by milling of a mixture of cobalt and boron powders

A. CORRIAS, G. ENNAS, G. MARONGIU, G. PASCHINA*
Dipartimento di Scienze Chimiche, Via Ospedale 72, 09124 Cagliari, Italy

A mixture of polycrystalline elemental cobalt and boron powders in the atomic ratio $Co_{67}B_{33}$ was mechanically milled for 150 h. The milled powders were examined by X-ray diffraction, extended X-ray absorption fine structure spectroscopy and differential scanning calorimetry. Two steps where energy was regulated by different full/void volume ratio in the vials were carried out. In the first milling step ($f/v = 1/1$) amorphization involves only a portion of the starting powder and reaches a steady state after 25 h. More energetic conditions ($f/v = 1/5$) lead to almost complete amorphization of the sample after 70 h, and in the final stages the formation of crystalline t-Co_2B is observed. Then a steady state, in which both amorphous and crystalline phases coexist, is reached.

1. Introduction

Several different methods have been developed so far for the preparation of amorphous metallic alloys; among them the rapid quenching of melts is widely adopted, and products in the form of splats, thin films, ribbons and wires are prepared by splat cooling and melt spinning [1]. Fine powders are also obtained via an ultrarapid quenching technique by melt atomization methods [1].

Melting is, however, not necessarily required: annealing at relatively low temperatures [2] and cold rolling [3] of multilayer polycrystalline materials as well as mechanical alloying of mixtures of elemental metal powders [4, 5] lead to the formation of amorphous alloys via solid-state amorphization reactions (SSAR). Anomalously fast diffusion of one element into the other as well as a large negative heat of mixing seem to be essential requirements in the systems reported so far as undergoing SSAR. Most of the systems studied refer to bimetallic alloys of one early and one late transition element and a few to metal–metalloid ones; among these metal–silicon amorphous alloys have been obtained by SSAR induced by multilayer annealing [6–9] and by mechanical alloying [10].

Solid-state amorphization of metal–boron systems seems to be more difficult [11]. On the other hand Me–B amorphous alloys in a wide range of compositions have been prepared by rapid quenching [12] and amorphous Me–B powders have been obtained by chemical reduction of metal ions in aqueous solutions [13, 14]. Recently an amorphous phase obtained in an Ni–B–Ni trilayer has been reported [15].

We report herewith amorphization by mechanical alloying of a $Co_{67}B_{33}$ mixture of the powdered elements. The atomic composition was chosen in order to keep the Co/B ratio close to that found in the

amorphous powders prepared by chemical reduction of Co^{2+} by KBH_4 [14].

2. Experimental procedure

2.1. Milling

A mixture of polycrystalline powders of cobalt (Ventron 99.8%, containing both h.c.p. α-Co and f.c.c. β-Co) and boron (Ventron 99.7%) in a weight ratio corresponding to a formal $Co_{67}B_{33}$ composition were milled in a planetary Fritsch Pulverisette 5 ball mill, with a balls/powder weight ratio around 5.5.

Tempered steel vials were sealed under pure argon in order to avoid oxygen contact; excessive heating was controlled by a cold air jet and by alternating milling and rest periods at 5 min intervals. The energy transfer to the system was regulated by the full/void volume ratio (f/v) in the vials; a low energy transfer step ($f/v = 1/1$) and a high one ($f/v = 1/5$) were successively carried out.

2.2. X-ray diffraction (XRD)

SSAR was followed by X-ray diffraction spectra obtained from small portions of the mixture, sampled at regular time intervals in a glove bag filled with argon. Spectra were recorded on a Seifert θ–θ diffractometer using MoK_{α} radiation in the angular range $2° \leqslant \theta \leqslant 22°$.

2.3. EXAFS

Extended X-ray absorption fine structure (EXAFS) spectra on the Co K-edge were collected on some of the samples used for XRD analyses. Data were collec-

---

*To whom correspondence should be addressed.

ted at the EXAFS-I beamline at LURE (Orsay) using synchrotron radiation produced by the DCI storage ring operating at 1.85 GeV and 200 mA; a channel-cut Si 331 monochromator was used.

2.4. Differential scanning calorimetry (DSC)

A portion of the sample which showed maximum amorphization (70 milling hours) was heated up to 500 °C in a DSC 7 Perkin-Elmer calorimeter, at a heating rate of 30 °C min^{-1} under an argon flux.

3. Results and discussion

The XRD pattern of the starting powder mixture is shown in Fig. 1a. Comparison of the intensities of the (2 0 0) peak due to f.c.c. β-Co [16] and of (1 0 0) and (1 0 1) peaks due to h.c.p. α-Co [17] indicates that β-Co, stable over 450 °C but still retained at room temperature, is quantitatively predominant; the remaining peaks of the two forms are mostly superimposed and are not discernible. No peaks ascribable to boron are evident, due both to its low weight content and to its small scattering factor.

Fig. 1b shows the spectrum of the sample after 10 h milling; h.c.p. resolved peaks, although broadened, maintain their original intensity. A definite intensity decrease is clearly evident for the (2 0 0) f.c.c. peak, indicating that the metastable phase is most affected in the early milling stages. This fact is also confirmed by the intensity drop of superimposed (0 0 2) h.c.p. and (1 1 1) f.c.c. peaks. The intensity variation is accompanied by the appearance at the bottom of the main

peaks of a halo which keeps increasing up to 25 milling hours; the prominent peaks remain present at their original angular positions, although they continue to broaden.

No significant variations were observed after a further 18 (43 total) milling hours (Fig. 1c), when Bragg peaks due to crystalline cobalt were still present.

At this point milling conditions were changed by increasing the collisional energy transfer in order to favour the amorphization progress. Since the angular rotation rate of the mill was close to maximum the sample and the balls were transferred to larger vials, thus lowering the full/void ratio to 1/5 and increasing the mean free path of the balls and therefore their kinetic energy.

After 27 (total 70) hours of further milling under the new operational conditions the sample reached an almost complete amorphization, as shown by the pertinent diffraction pattern (Fig. 1d); here the amorphous halo is predominant and Bragg peaks are barely discernible. Milling was continued but no progress in amorphization, as inferred from the area of the halo, was estimated; Bragg peaks of a crystalline phase, lately identified as t-Co_2B [18], started instead to appear. Their peak intensity reaches a maximum which is that shown in the diffraction pattern obtained after a total of 150 milling hours (Fig. 1c). The t-Co_2B peaks are broadened, indicating that its crystallites remain rather small as an effect of milling, which hampers their growth. The amorphous halo shows neither a significant flattening nor a widening with respect to that in Fig. 1d.

Fig. 2 shows the spectra of the sample at the end of the milling process (150 h) as well as those which result after thermal treatments. These show that the intensities of both t-Co_2B and f.c.c. β-Co peaks increase with temperature.
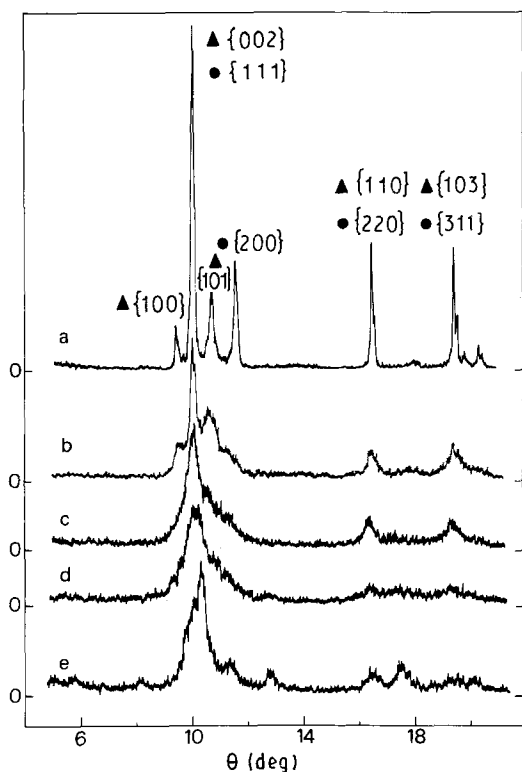

Figure 1 X-ray diffraction spectra (MoK_α) for (a) starting powder, and samples milled for (b) 10, (c) 43, (d) 70 and (e) 150 h (arbitrary intensity units). (▲) h.c.p. α-Co, (●) f.c.c. β-Co.
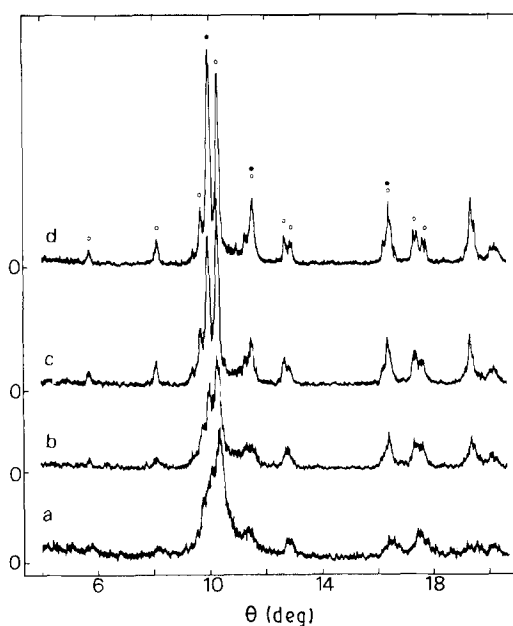

Figure 2 X-ray diffraction spectra (MoK_α) for (a) as-prepared final milling product, and after thermal treatment at (b) 300, (c) 400 and (d) 500 °C (arbitrary intensity units). (●) β-Co, (○) Co_2B.

Fourier transform moduli of EXAFS interference functions from samples milled for 15, 43 and 70 h are reported in Fig. 3a–c, together with that from an f.c.c. β-Co (Fig. 3d) reference foil. The $F(r)$ of the f.c.c. Co sample differs significantly from that reported for h.c.p. Co [19] in the range 0.43–0.52 nm, where the f.c.c. structure shows an extraordinarily intense peak due to a focusing effect of the fourth shell [20].

$F(r)$ functions of the samples after 15 and 43 milling hours (Fig. 3a and b, respectively) are very similar; both show a drop, more evident at large distances, in the area of all the peaks with respect to their crystalline counterparts. This fact confirms the X-ray results that early milling stages lead rapidly to a partial demolition of the crystalline network followed by a stationary state, when amorphization is far from being complete.

The more energetic conditions of the second milling step lead to a final product which gives an interference function and an $F(r)$ much closer to those exhibited by amorphous alloys of similar composition obtained by melt-spinning and chemical reduction [21, 22]. All show a large peak centred at about 0.2 nm like that in Fig. 3c. Some weak extra peaks present in the milled sample, particularly that centred at 0.46 nm, suggests that the small fraction of crystalline cobalt still present is due to f.c.c. phase.

Fig. 4 shows the DSC trace from the 70 h milled sample. It has two significant peaks: the first, rather small, around 300 °C can be ascribed to the growth of cobalt crystallites which did not take part in the solid-state reaction. This hypothesis is confirmed by the X-ray spectrum of the sample heated up to 330 °C and
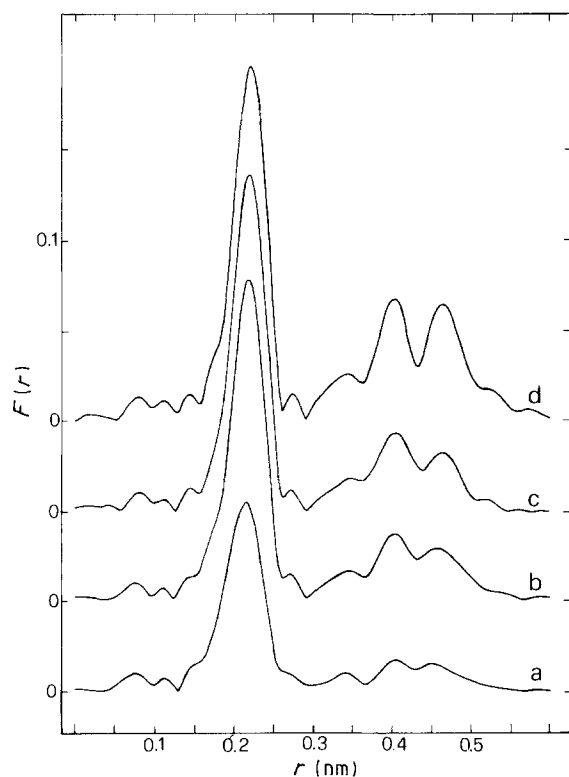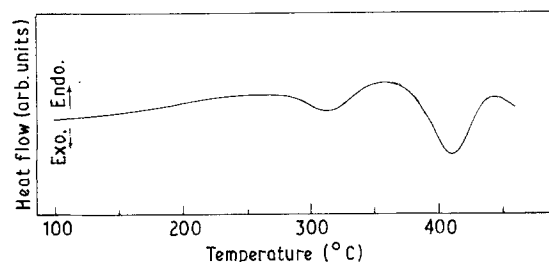

Figure 4 DSC trace for 70 h milled sample.
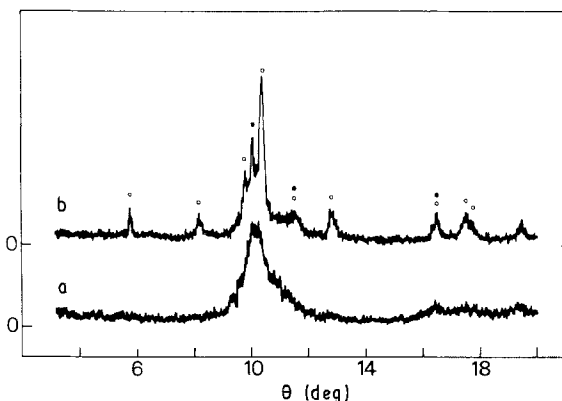

Figure 5 X-ray diffraction spectra for (a) 70 h milled sample and (b) after DSC analysis carried out up to 500 °C (arbitrary intensity units). (●) β-Co, (○) Co_2B.

then rapidly quenched; it shows the reappearance of a faint peak at $\theta = 10°$ common to the two phases of metallic cobalt.

The second and larger DSC peak is mainly due to the crystallization of t-Co_2B and partially to the h.c.p.–f.c.c. transition of metallic cobalt; this is confirmed by the XRD spectrum of the sample heated up to 500 °C, which shows a peak at $\theta = 11.5°$ due to the (2 0 0) f.c.c. cobalt reflection (Fig. 5).

The following sequence of events seems to be consistent with the experimental facts reported above. In the beginning the cobalt and boron crystalline powders are intimately crushed and their surface contact is therefore enlarged; this is followed by the diffusion of the smaller species (B) into the larger one (Co), with a consequent disordering of its crystalline lattice, in agreement with the mechanism suggested to explain the solid-state amorphization reaction in analogous systems [15, 23]. Afterwards the amorphous phase increases amid the component layers and at their expense, as supported by the broadening and lowering in intensity of the crystalline cobalt peaks; these, on the other hand, do not shift from their angular positions, excluding the formation of any crystalline solid solution.

The amorphous phase increases up to a maximum when its own presence becomes a barrier to the further diffusion of boron; diffusion is hampered by the absence in the amorphous state of point and line defects and of grain boundaries. A similar behaviour has been observed in an Ni–B multilayer [15], where the amorphous phase does not grow beyond a 40 nm thickness.

Figure 3 EXAFS $F(r)$ for samples milled for (a) 15, (b) 43 and (c) 70 h, and for (d) f.c.c. β-Co reference foil. N. B. The intensity of (d) is reduced by a factor of two.

When milling is restarted under more energetic conditions the barrier which opposed the diffusion of boron is overcome, and the amorphous phase keeps growing up to a point when the presence of crystalline cobalt is barely detectable both in XRD and EXAFS spectra.

The higher kinetic energy associated with the balls also helps the diffusion of the host element (Co) and produces proper conditions for the formation of crystalline t-Co$_2$B [23]. Then a steady state is reached in which both amorphous and crystalline phases coexist.

Acknowledgement

References

1. F. E. LUBORSKY (ed.), "Amorphous Metallic Alloys" (*Butterworth*, 1983).
2. R. B. SCHWARZ and W. L. JOHNSON, *Phys. Rev. Lett.* **51** (1983) 415.
3. M. ATZMON, J. VERHOEVEN, E. GIBSON and W. L. JOHNSON, *J. Appl. Phys.* **58** (1985) 3865.
4. C. C. KOCH, O. B. CAVIN, C. G. McKAMEY and J. O. SCARBROUGH, *Appl. Phys. Lett.* **43** (1983) 1017.
5. R. B. SCHWARZ, R. R. PETRICH and C. K. SAW, *J. Non-Cryst. Solids* **76** (1985) 281.
6. D. M. VANDERWALKER, *Appl. Phys. Lett.* **48** (1986) 707.
7. M. NATAN, *ibid.* **49** (1986) 257.
8. K. HOLLOWAY and R. SINCLAIR, *J. Appl. Phys.* **61** (1987) 1359.
9. I. J. M. N. RAAIJMAKERS, A. H. READER and P. H. OOSTING, *ibid.* **63** (1988) 2790.
10. N. BURGIO, G. ENNAS, M. MAGINI, F. PADELLA, B. SCHIPPA and P. SUSINI, in "Solid State Powder Processing", edited by A. H. Clauer and J. J. de Barbadillo (Mineral, Metals & Materials Society, 1990) p. 344.
11. B. M. CLEMENS and J. J. NEUMEIER, *J. Appl. Phys.* **58** (1985) 4061.
12. T. GUO-HUA and C. WAN-RONG, *Mater. Sci. Eng.* **97** (1988) 329.
13. S. WELLS, S. W. CHARLES, S. MORUP, S. LINDEROTH, J. van WONTERGHEM, J. LARSEN and M. B. MADSEN, *J. Phys. Condens. Matter* **1** (1989) 8199.
14. A. CORRIAS, G. ENNAS, G. LICHERI, G. MARONGIU, and G. PASCHINA, *Chem. Mater.* **2** (1990) 363
15. A. N. CAMPBELL, J. C. BARBOUR, C. R. HILLS and M. NASTASI, *J. Mater. Res.* **4** (1989) 1303.
16. ASTM Card N 15-806.
17. ASTM Card N 5-727.
18. ASTM Card N 3-878.
19. C. BROUDER, G. KRILL, E. DARTYGE, A. FONTAINE, G. MARCHAL and P. GUILMIN, *J. Physique C8* **12** (1986) 1065.
20. B. K. TEO, *J. Amer. Chem. Soc.* **103** (1981) 3990.
21. J. M. DUBOIS, G. Le CAER, P. CHIEUX and J. GOULON, *Nucl. Instrum. Meth.* **199** (1982) 315.
22. A. CORRIAS, G. LICHERI, G. PASCHINA, and G. VLAIC, *SIF Conf. Proc.* **25** (1990) 683.
23. K. SAMWER, *Phys. Rep.* **161** (1988) 1.